

# Relationship between CME Parameters and Large-Scale Structure of Solar Magnetic Fields

V.G. Fainshtein<sup>1</sup>, E.V. Ivanov<sup>2</sup>

<sup>1</sup> Institute of Solar-Terrestrial Physics, Siberian Department,  
Russian Academy of Sciences, Irkutsk, Russia

E-mail: vfain@iszf.irk.ru

<sup>2</sup> Pushkov Institute of Terrestrial Magnetism, Ionosphere, and Radio Wave Propagation,  
Russian Academy of Sciences, Troitsk, Moscow Region, Russia

E-mail: eivanov@izmiran.ru

Accepted: 19 December 2009

**Abstract.** In this work, we explore how the parameters of coronal mass ejections (CME) associated with eruptive prominences (EP) depend on their position relative to the coronal streamer belt (CSB) and coronal streamer chains (CSCs). We show that the CMEs whose axes are close to CSB propagate at lower mean speed than the CMEs observed in the vicinity of CSCs. The CMEs concentrated at CSCs have larger mean kinetic energy than those associated with CSB. The mean mass is maximum for the events associated with CSB and minimum for events observed near the base of open magnetic field configurations (OMF) - counterparts of coronal holes. The mean angular size is virtually the same for the CMEs of both types. The CME deviation from the radial trajectory has been studied. It is shown that CMEs may deviate noticeably from the radial propagation both on their way from the origin site (prominence eruption site) up to about 2.5 solar radii ( $R_0$ ) and farther, from  $\sim 2.5$  up to  $20 R_0$ . In the epoch of solar minimum and at the rise of the cycle, the deviation in the first part of the trajectory (up to  $2.5 R_0$ ) is mainly towards the equator. In the other phases, no preferable direction has been revealed. As the EP latitude increases up to  $\pm 45^\circ$ , the CME deviation, on the average, increases, too. It is shown that about 50% of all CMEs change the sense of deviation when passing from the near-solar part of the trajectory to its far part so that, as the CME moves away from the Sun, its propagation becomes more radial. The results obtained show that large-scale solar magnetic fields have a significant effect on the characteristics and propagation of coronal mass ejections.

© 2010 BBSCS RN SWS. All rights reserved

**Keywords:** eruptive prominence, coronal mass ejection, large-scale magnetic field

## Introduction

It is well known [1] that CMEs concentrate in the vicinity of the neutral line (NL) of the magnetic field on the source surface (sphere of radius  $R=2.5R_0$ , where  $R_0$  is the solar radius) calculated under potential approximation from the coronal field data. It is shown that this line coincides with the base of the coronal streamer belt (CSB) (e.g., see [2]). A detailed analysis has revealed another site in the corona where CME events are observed frequently, namely, the coronal streamer chains (CSCs) [3]. CSCs separate coronal holes or open magnetic fields of like polarity [2], while the CSB separates the fields of opposite polarity (Fig.1). The shape and position of CSCs in the corona (including the source surface) can also be calculated from the coronal field data [2]. As the solar maximum approaches, the fraction of CME events concentrated at CSCs increases [3, 4]. As shown in [4, 5], the properties of the CMEs that occur near the CSB and CSCs may differ. According to [4], the CMEs whose axes are close to the source-surface neutral line are usually broader and faster. In [5], it is shown that the CMEs that occur at the base of the streamer belt cause stronger effect on the Earth than those formed near the streamer chains.

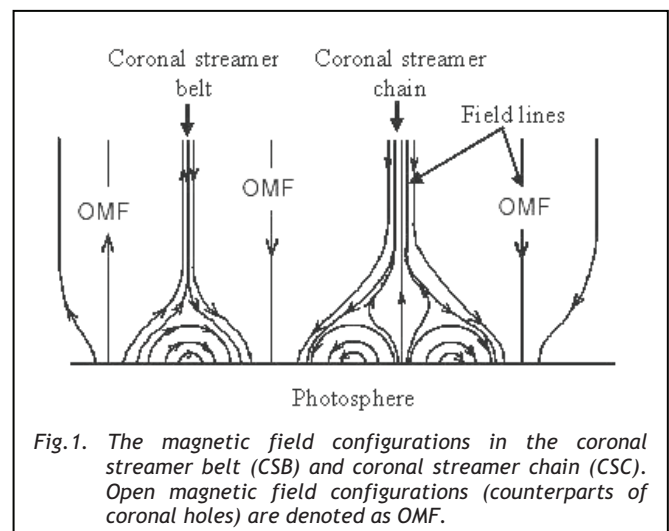
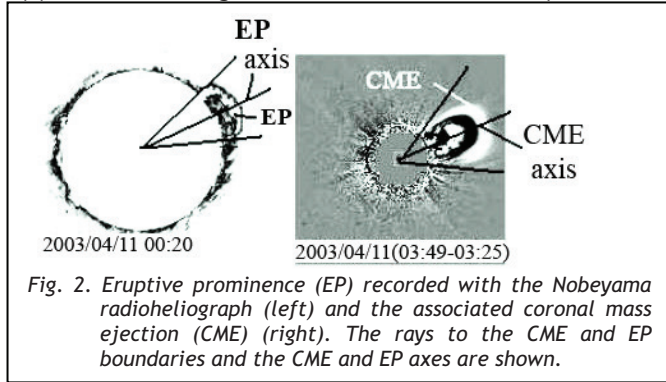


Fig.1. The magnetic field configurations in the coronal streamer belt (CSB) and coronal streamer chain (CSC). Open magnetic field configurations (counterparts of coronal holes) are denoted as OMF.

In this work, we continue to study the parameters of CME events depending on the position of their axes relative to the CSB or CSCs and the peculiarities of CME deviation from the radial trajectory at different distances from the Sun.

**Database**

We have analyzed 214 CME events associated with eruptive prominences for 1997-2006 from the Large Angle and Spectrometric Coronagraph (LASCO) CME list [6] (e.g., see Fig. 2). These events were chosen because (1) EP is a good indicator of the CME source position in latitude (see below) and (2) the CMEs associated with EPs are located in the immediate vicinity of the plane of the sky, minimizing the projection effects on the apparent CME angular width and front velocity.



Besides, we considered the EP-associated CMEs recorded in radiofrequency range with the Nobeyama radioheliograph and the events observed in H-alpha (EPL). In the former case, we used the data from Table 1 in [7] and from the list of «Limb events of Nobeyama radioheliograph» [8]. In the latter, the information on eruptive limb prominences (EPL) was obtained from SGD [9].

The CME parameters (velocity, angular width, axis position angle, mass, and kinetic energy) were taken from the LASCO CME list [6]. The linear fit velocity was used as the CME velocity.

The CME events were chosen following the criteria listed below:

- 1) The CME was first recorded in the LASCO C2 field of view not earlier than one hour and not later than three hours after the prominence eruption.

- 2) The difference between the CME and EP position angles was no more than  $\pm 50^\circ$  (no more than  $\pm 60^\circ$  in three cases when additional criteria were used).

- 3) The angular width was no more than  $180^\circ$  (for all CME events but one). Most of the chosen CMEs contained a feature, which is usually identified as EP.

The coronal magnetic field used for the analysis was calculated under potential approximation from Wilcox Solar Observatory (WSO)/Stanford synoptic maps of photospheric magnetic fields by the method developed at IZMIRAN [10]. Examples of the calculated field structure in the corona are illustrated in Fig.3. The solid bold line is the neutral line of the source surface magnetic field, which marks the base of the coronal streamer belt. The dotted lines mark the source-surface counterpart for the coronal streamer chains, which separate two adjacent open magnetic fields (OMF) of the same polarity. The small filled circles denote the sites on the solar surface where eruptive prominences were observed; the large filled circles are the projections of CME axes onto the source surface as inferred from the LASCO C2 observations.

**Relationship between the CME parameters and large-scale structure of solar magnetic fields**

A comparative analysis of the large-scale magnetic features and CMEs in the corona has revealed two types of CME events depending on the position of their axes relative to the neutral line of the source-surface magnetic field (coronal streamer belt, CSB) or the lines, separating two adjacent open magnetic field configurations of the same polarity (coronal streamer chains, CSCs) (see also [3, 4]).

Fig.4a represents the distribution of CME events in accordance with their distance from the CSB and the nearest CSC. The line passing through the zero point at equal distances from the coordinate axes divides all CMEs into two groups: the events that occur in the vicinity of the CSB (above the line) and those that occur near CSCs (below the line).

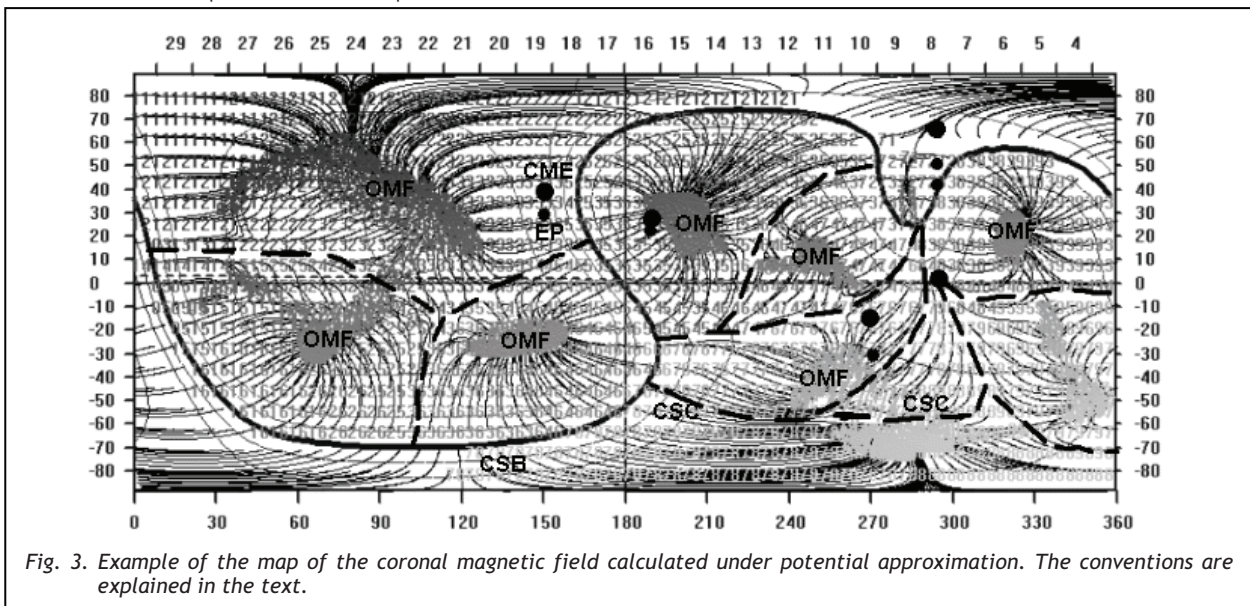


Fig. 3. Example of the map of the coronal magnetic field calculated under potential approximation. The conventions are explained in the text.

One can see that most of the events observed closer than 30 degrees to the neutral line belong to the CME group associated with the CSB, while the events observed farther than 30 degrees from the neutral line belong to the CME group associated with CSCs.

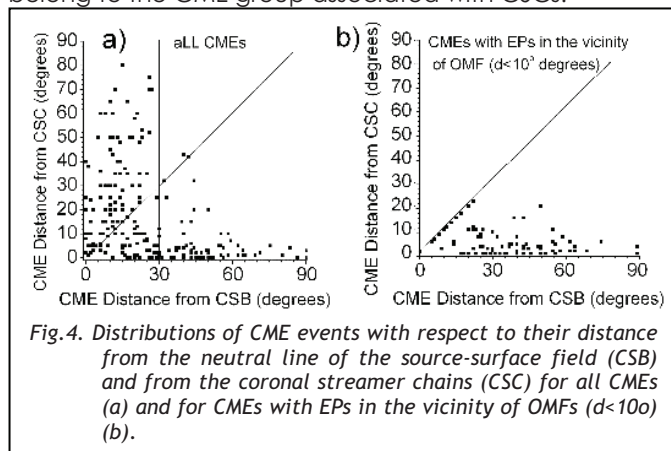


Fig.4. Distributions of CME events with respect to their distance from the neutral line of the source-surface field (CSB) and from the coronal streamer chains (CSC) for all CMEs (a) and for CMEs with EPs in the vicinity of OMFs ( $d < 10^\circ$ ) (b).

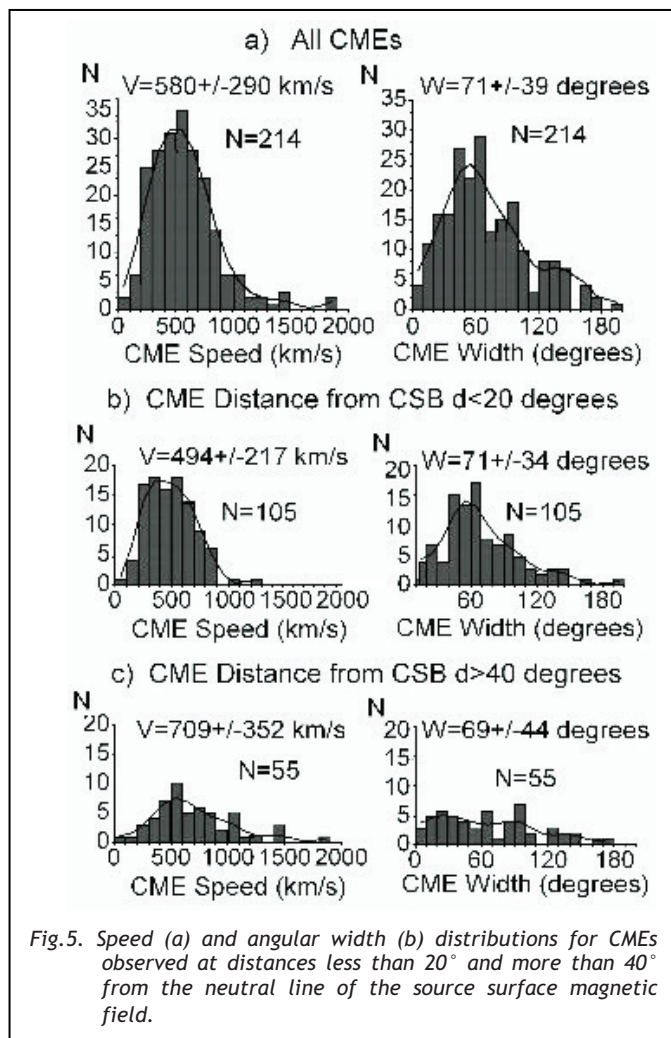


Fig.5. Speed (a) and angular width (b) distributions for CMEs observed at distances less than  $20^\circ$  and more than  $40^\circ$  from the neutral line of the source surface magnetic field.

We also isolated a group of EP-associated CME events observed near the base of open magnetic configurations (counterparts of coronal holes) no farther than at  $10^\circ$  from their boundaries. All such events turned out to belong to the group associated with CSCs (Fig.4b).

Fig. 5 shows the CME distributions according to their speeds and angular dimensions for all events under examination (a) and for the CMEs observed at the distances  $d < 20^\circ$  (b) and  $d > 40^\circ$  (c) from the source-surface neutral line. Group (b) consists mainly of CMEs associated with the CSB (CSB group), while the CMEs associated with CSCs form CSC group (c). It is readily seen that the latter are, on the average, faster.

Taking into account the r.m.s. scatter of the velocity and number of the events of each type, it can be shown with a probability no less than 0.95 that the mean CME velocities in these two groups are, actually, different. In other words, the velocity difference between the two CME groups is statistically significant.

A detailed analysis has shown that the mean velocity of CMEs observed at an angular distance  $d$  smaller than the boundary distance  $d_B$  from CSB increases with the increase of  $d_B$ .

On the other hand, the difference between the mean angular dimensions  $W$  of the CSB- and CSC-group CMEs in Fig. 5 is small and statistically insignificant.

The CMEs concentrated at CSCs have larger mean kinetic energy than those associated with CSB (see Table 1). The mean mass is maximum for the events associated with the CSB and minimum for the OMF-group events. The mass and kinetic energy values were taken from the LASCO CME list [6].

The mean velocity of CMEs observed in the vicinity of open magnetic configurations (coronal holes) is comparable with the mean CSC-group velocity and, thus, it exceeds the mean velocity of CMEs associated with the CSB. These CMEs have also smaller mean mass and somewhat smaller kinetic energy than the CSC-group events.

The results obtained are summarized in Table 1.

### Deviation of the CME trajectory from radial direction during CME propagation from the Sun

Let us assume that all analyzed CMEs associated with EPs occur in the immediate vicinity of the EP axes (at least in latitude). This assumption is based on the inspection of SOHO [12, 13] and Mark3, 4 (Mauna Loa Solar Observatory, MLSO) images on which the CME events observed at short distances from the Sun ( $R < 2R_o$ ) are close in latitude to the respective EPs. We have compared the positions of the axes of the EPs and associated CMEs in the field of view of the Mark 3, 4 coronagraphs (MLSO) in the cases when the CME front was at  $R \leq 1.7R_o$  from the disk center. The analysis was performed for a limited number of the events, which were partly taken from our list and partly (20 CMEs) randomly chosen from the Mark 3, 4 data for the period 1997-2006 (most CME observations did not coincide with the Mark 3, 4 operation periods). As shown by the analysis, the positions of the EP and CME axes do not differ by more than  $10^\circ$  for most events under consideration. The r.m.s. scatter of deviation of the CME axis from EPs is  $\approx 7^\circ$ . The CME and EP axes were determined as bisecting lines between the rays from the disk center to the boundaries of CME or EP at the eruption start time (Fig. 2). This allows us to suggest that the distance in latitude between EP and the CME in the

**TABLE 1**  
Mean velocity, angular width, mass, and kinetic energy of CME events

	all CMEs	CSB Group	CSC Group	CMEs near OMF
Number of events	214	100	114	98
Mean velocity (km/s)	580±290	509±230	643±322	644±330
Mean angular width	71°±39°	75.6°±38.4°	72.4°±43.2°	67.6°±39°
Mean mass (g)	(5.6±1.2)×10 <sup>15</sup>	(5.9±1.0)×10 <sup>15</sup>	(5.3±1.2)×10 <sup>15</sup>	(4.9±1.2)×10 <sup>15</sup>
Mean kinetic energy (erg)	(1.6±1.2)×10 <sup>31</sup>	(1.1±0.97)×10 <sup>31</sup>	(2.3±1.7)×10 <sup>31</sup>	(1.8±1.4)×10 <sup>31</sup>

field of view of LASCO C2 more than 7°-10° is due to the CME deviation from radial trajectory. Hence, in most cases under discussion, the deviation can be determined to an accuracy ≤7°-10°. Note that we are dealing with the latitude of the axis of EP image in the plane of the sky obtained as a result of projection of the real filament onto this plane.

Earlier in [7, 13] it was shown that CMEs associated with EPs might depart from the radial trajectory both towards and away from the equator.

also the latitude of intersection of the CME axis with the source surface at RS=2.5Ro. The part of the trajectory of CME from its origin to the appearance in the field of view of LASCO C2 will be regarded as the path to the source surface (a sphere of radius RS=2.5Ro). Positive differences (Lat EP - Lat CME2.5Ro) and (Lat CME2.5Ro - Lat CME20Ro) correspond to deviation of CME trajectories towards the equator and negative ones, to deviation towards the pole. Since the directions towards the equator and towards the pole in the southern hemisphere are opposite to the analogous directions in the northern hemisphere, the differences (Lat EP - Lat CME2.5Ro) and (Lat CME2.5Ro - Lat CME20Ro) in the southern hemisphere were taken with the opposite sign.

Fig. 6 illustrates a noticeable deviation of CMEs from the radial direction along both parts of the trajectory. One can see that the largest deviation occurs on the path from the CME origin to the source surface (Fig. 6a). It is also to be noted that in the period from 1997 to June 1999 (the minimum and rise phase of the solar cycle), the deviation on this path was mainly towards the equator (Lat EP - Lat CME2.5Ro) > 0. A similar result had been obtained earlier in [7] for the period 1997-2001. Beginning with July 1999 and approximately up to 2005 (the maximum and decline of activity), no preferable direction of deviation was identified.

Fig. 7 illustrates the variation of CME trajectory from the origin (filament eruption site) to the first appearance in the LASCO C2 field of view at 2.5Ro and farther, up to 20Ro. The same as in Fig. 6, the positive differences (Lat EP - Lat CME2.5Ro) and (Lat CME2.5Ro - Lat CME20Ro) correspond to the deviation towards the equator and the negative ones, to the pole. For the southern hemisphere, the differences (Lat CME2.5Ro - Lat CME20Ro) and (Lat CME2.5Ro - Lat CME20Ro) are taken with the opposite sign. One can see that the CMEs that occur at low latitudes deviate mainly to the poles and then, as the latitude increases, the deviation to the equator becomes predominant (Fig. 7a). There is also another regularity that can be inferred from Fig. 7a. As the EP latitude increases up to ±45°, the CME deviation, on the average, increases, too. This is most clearly pronounced for the CMEs deviating to the equator.

The CMEs observed at the source surface at low latitudes are associated with EPs, which occurred on more high latitudes and then their deviations from the occurrence site to the source surface correspond to deviations towards the equator. As the CME latitude at the source surface increases, the deviation towards the poles begins to prevail (Fig. 7b).

Similar regularities are also observed along the second part of the CME trajectory from 2.5Ro up to 20Ro

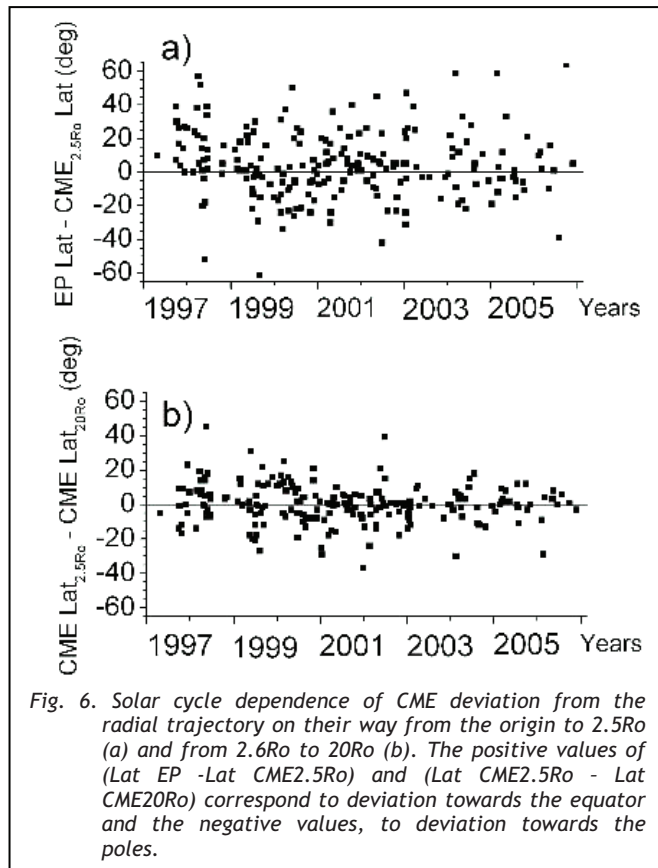


Fig. 6. Solar cycle dependence of CME deviation from the radial trajectory on their way from the origin to 2.5Ro (a) and from 2.6Ro to 20Ro (b). The positive values of (Lat EP - Lat CME2.5Ro) and (Lat CME2.5Ro - Lat CME20Ro) correspond to deviation towards the equator and the negative values, to deviation towards the poles.

Fig. 6 illustrates variations in the latitude difference between the EP and CME in the LASCO C2 field of view (CME2.5Ro Lat) (a) and between the CMEs at the distances of 2.5Ro (CME2.5Ro Lat) and 20Ro (CME20Ro Lat) from the Sun (b) during solar cycle 23. By the CME and EP latitudes, we mean the latitudes of their axes. For the EP recorded in radiofrequency range, the latitude was found directly from its image at the eruption start time. For the EP recorded in H-alpha (EPL), it was taken from SGD [9]. The latitude of CME axis in both cases was derived from the CME position angle given in the catalogue [6]. The convention CME2.5Ro Lat denotes

(Fig. 7c,d). The only exception is an extremely weak latitudinal dependence of deviations of CMEs observed at  $R=2.5R_o$  (Fig. 7c).

The CME deviation to the equator along the first part of the trajectory may be explained by the effect of the coronal streamer belt, which also tends to the equator at these distances from the Sun. The detailed mechanism is discussed in [13].

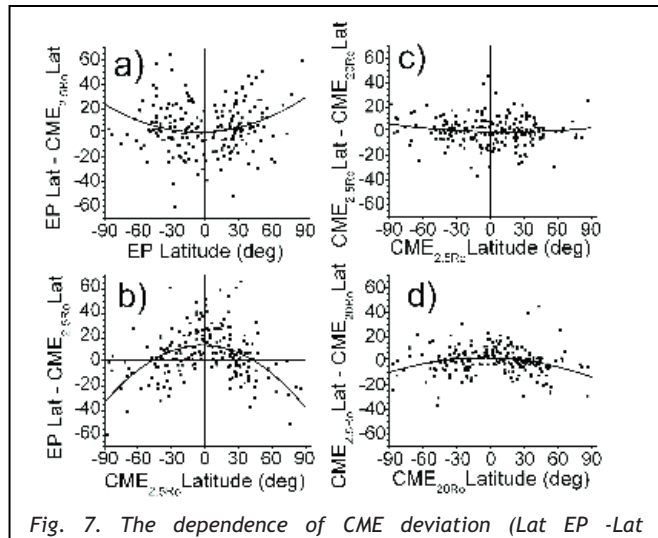


Fig. 7. The dependence of CME deviation (Lat EP -Lat CME2.5Ro) on the latitude of EP (EP Lat) (a) and CME2.5Ro (Lat CME2.5Ro) (b) at the initial stage of propagation (up to  $R=2.5R_o$ ) and a similar dependence of deviation (Lat CME2.5Ro - Lat CME20Ro) on the CME latitude at  $R=2.5R_o$  (Lat CME2.5Ro) (c) and at  $R=20R_o$  (Lat CME20Ro) (d). The positive differences (Lat EP -Lat CME2.5Ro) and (Lat CME2.5Ro - Lat CME20Ro) correspond to deviation towards the equator and the negative ones, to deviation towards the poles.

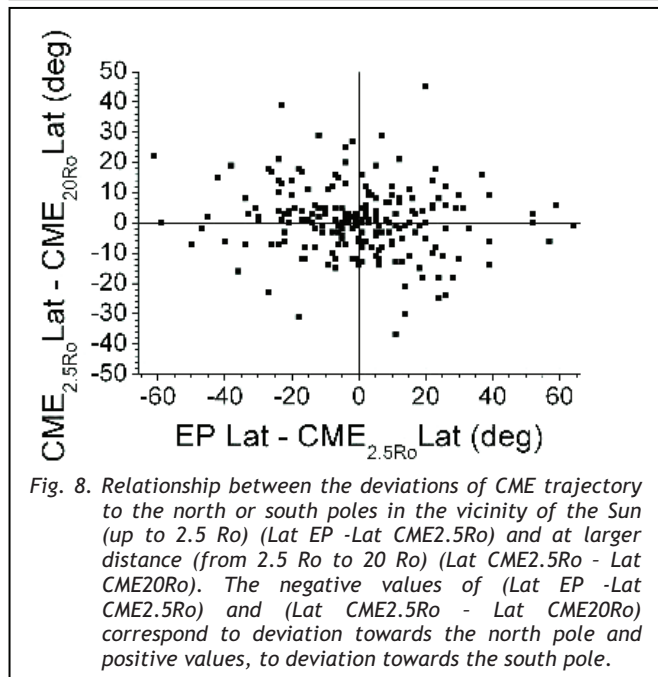


Fig. 8. Relationship between the deviations of CME trajectory to the north or south poles in the vicinity of the Sun (up to  $2.5 R_o$ ) (Lat EP -Lat CME2.5Ro) and at larger distance (from  $2.5 R_o$  to  $20 R_o$ ) (Lat CME2.5Ro - Lat CME20Ro). The negative values of (Lat EP -Lat CME2.5Ro) and (Lat CME2.5Ro - Lat CME20Ro) correspond to deviation towards the north pole and positive values, to deviation towards the south pole.

Fig. 8 illustrates the relationship between the CME deviations from radial propagation along the near-solar (Lat EP - Lat CME2.5Ro) and far (Lat CME2.5Ro - Lat CME20Ro) parts of their trajectory. In this figure the

negative differences (Lat EP -Lat CME2.5Ro) and (Lat CME2.5Ro - Lat CME20Ro) correspond to deviation towards the north pole and the positive ones, to deviation towards the south pole regardless of the hemisphere the CMEs originate in. If (Lat EP -Lat CME2.5Ro) and (Lat CME2.5Ro - Lat CME20Ro) have different signs, the CMEs reverse the sense of deviation when passing from the first to the second part of their propagation trajectory. This change occurs in about 50% of cases and is such that the CME propagation in the far part of the trajectory becomes more radial than in the initial part.

Table 2 provides the mean deviations along both parts of the CME trajectory for the period 1997-2006 separately for the CSB-, CSC-, and OMF-group events. Averaged were the absolute values without taking into account the sense of deviation. One can see that the mean deviation values in all three groups do not differ significantly.

### Conclusions

1. All eruptive CME events can be divided into two groups according to their distance from the neutral line of the source surface magnetic field. One group comprises the CMEs whose axes are at a distance less than  $30^\circ$  from the source-surface neutral line and another, the CMEs whose axes are farther than  $30^\circ$  from the neutral line. The former are the events that occur at the base of the coronal streamer belt (CSB-group CMEs). The events of another group (CSC-group CMEs) occur in the vicinity of the coronal streamer chains. The CME events whose sources (EPs) were recorded at distances no more than  $10^\circ$  from the OMF boundaries (OMF-group events) fall in the CSC group.

2. As the CME distance from the neutral line increases, their mean velocity and kinetic energy grow, being the largest for the events associated with the coronal streamers chains, while the angular size changes little. As the CME distance from the neutral line increases, their mean velocity and kinetic energy grow, being the largest for the events associated with the coronal streamers chains, while the angular size changes little. The mean mass is maximum for the events associated with the coronal streamer belt and minimum for the OMF-group events. These latter have approximately the same mean velocity but somewhat smaller kinetic energy and mass than the other CSC-group events. This may be due to more favorable generation and propagation conditions in the vicinity of open magnetic fields [14].

3. Most CMEs deviate rather noticeably from the radial trajectory as they propagate from the photosphere to the source surface and farther, up to 20 solar radii. At the minimum and in the rise phase of the solar cycle (1997-1999.5), the CME deviation at the early stage of propagation (up to  $2.5 R_o$ ) is mainly towards the equator, while at the following phase of the cycle, no preferable direction can be identified. This result is consistent with previous studies on the deviation.

4. As the EP latitude increases up to  $\pm 45^\circ$ , the CME deviation, on the average, increases, too. This is most clearly pronounced for the CMEs that deviate to the equator.

**TABLE 2**  
**Mean deviations of CMEs from the radial trajectory at the distances Ro-2.5Ro and 2.5Ro-20Ro from the Sun**

	All CMEs	CSB Group	CSC Group	CMEs near OMF
<b>Number of events</b>	214	100	114	98
<b>Ro - 2.5Ro</b>	15.3°±13.6°	14.0°±12.3°	16.2°±16.9°	16.4°±15.2°
<b>2.5Ro - 20Ro</b>	8.1°±7.8°	8.2°±7.9°	8.2°±7.9°	8.1°±8.8°

5. About 50% of all events under consideration change the sense of deviation when passing from the first part of their trajectory to the second one in such a way that the propagation becomes more radial. This may imply that the deviation on two parts of the trajectory is determined by different physical mechanisms.

The results obtained show that large-scale solar magnetic fields have a significant effect on the characteristics and propagation of coronal mass ejections.

It should be emphasized that the regularities found in this work apply to the coronal mass ejections associated with eruptive prominences. The properties of the CMEs caused by other active events in the Sun will be discussed in our next work.

#### Acknowledgments

In this work, we have used SOHO/LASCO and Nobeyama data from the Internet and SGD data on eruptive prominences. The work was supported by the Russian Foundation for Basic Research (Project № SS-2258.2008.2 – Leading Scientific Schools) and the Program of Fundamental Research of the Presidium RAS P-16.

#### References

- [1] Mendoza, B., and Perez-Enriquez R., "Association of coronal mass ejections with the heliomagnetic current sheet", *J. Geophys. Res.*, 1993, vol. 98, pp. 9365-9370.
- [2] Eselevich V.G., V.G. Fainshtein, and G.V. Rudenko, "Study of the structure of streamer belts and chains in the solar corona", *Solar Phys.*, 1999, vol. 188, pp. 277-297.
- [3] Eselevich, V. G., "New results on the site of initiation of coronal mass ejections", *Geophys. Res. Lett.*, 1995, vol. 22, pp. 2681-2684.
- [4] Fainshtein V.G., "An investigation of solar factors governing coronal mass ejections characteristics". *Solar Phys.*, 1997, vol. 174, pp. 413-435.
- [5] Zhao X.P., Webb D.F., "Source regions and storm effectiveness of frontside full halo coronal mass ejections", *J. Geophys. Res.*, 2003, vol. 108, No. A6.1234, doi:10.1029/2002JA009606.
- [6] Gopalswamy N., Yashiro S., Michalek G., Stenborg G., Vourlidas A., Freeland S., Howard R., "Coronal mass ejections, Flares, Geomagnetic storms, Solar energetic particle events", *Earth, Moon, and Planets*, vol. 104, Issue 1-4, pp. 295-313 (<http://cdaw.gsfc.nasa.gov/CMElist>)
- [7] Gopalswamy N., M. Shimojo, W. Lu, S. Yashiro, K. Shibasaki, and R.W. Howard, "Prominence eruptions and coronal mass ejection: a statistical study using microwave observations", *Ap. J.*, 2003, vol. 586, pp. 562-578.
- [8] <http://solar.nro.nao.ac.jp/norh/html/prominence/>
- [9] <http://sgd.ngdc.noaa.gov/sgd/jsp/solarindex.jsp/>
- [10] Bugaenko O.I., Grechnev V.V., Zhigalkin R.K., Ignat'ev A.P., Kuzin S.V., Livshits I.M., Maksimov V.P., Obridko V.N., Pertsev A.A., Rudenko G.V., Slemzin V.S., Stepanyan N.N., Kharshiladze A.F., "Study of solar features based on complex ground-based and KORONAS-F observations: 1. Methods of observation and analysis of solar images obtained in different spectral bands", *Izv. Krymskoi Astrofizicheskoi observatorii (Notices of Crimean Astrophys. Obs.)*, 2004, vol. 100, pp. 110-122.
- [11] Plunkett, S. P., Brueckner, G. E., Dere, K. P. et al., "The relationship of green-line transients to white-light coronal mass ejections", *Solar Phys.*, 1997, vol. 175, pp. 699-718.
- [12] Plunkett S.P., Vourlidas A., Simberova S., Karlicky M., Kotrc P., Heinzel P., Kupryakov Yu.A., Guo W.P., Wu S.T. "Simultaneous SOHO and ground based observations a large eruptive prominence and coronal mass ejection", *Solar Phys.*, 2000, vol. 194, pp. 371-391.
- [13] Fainshtein V.G., "Some regularities in the relationship of limb coronal mass ejections with eruptive prominences and post-eruptive arcades", *Cosmic Research*, 2007, vol. 45, pp. 384-392.
- [14] Webb D.F., Nolte J.T., Solodina C.V., McIntosh P.S., "Evidence linking coronal transients to the evolution of coronal holes", *Solar Phys.*, 1978, vol. 58, pp. 389-396.